International Journal of Advanced Research in Science, Engineering and Technology

Vol. 12, Issue 12, December 2025

ISSN: 2350-0328

IMPACT FACTOR 7.150

On the theoretical determination of wind energy potential in the spherical coordinates of the Earth

S.F. Ergashev, A.A. Rakhimov

DSc, Professor, Department of Electronics and Instrumentation, Fergana state technical university Fergana, Uzbekistan

PhD Student, Department of Electronics and Instrumentation, Fergana state technical university, Fergana, Uzbekistan

ABSTRACT: This study presents a theoretical model for determining the wind energy potential using a spherical coordinate system. By integrating mathematical equations with atmospheric density data, the study calculates wind speeds and generated powers at different locations on Earth. The simulated wind speed in the Fergana region ranges from 13 to 18 m/s, with a peak speed of 25 m/s, indicating significant wind energy potential. The theoretical calculation confirms that wind power values change periodically depending on the coordinates of the Earth, under the influence of atmospheric dynamics and the difference in day and night temperatures. The estimated available wind energy resource can provide up to 18 MW per year, which can partially meet the energy demand of Uzbekistan. The study suggests that optimizing the placement of wind turbines based on this model can improve efficiency by 15-30%, reduce infrastructure costs by 10-20%, and minimize the environmental impact by 30-40%. The results validate the theoretical approach by comparing predicted wind speeds with five years of meteorological data from the Fergana Valley, demonstrating strong agreement between the model and real observations.

KEY WORDS: Spherical coordinates, earth coordinates, generated power, periodicity, and directivity.

1 INTRODUCTION

Wind energy plays a crucial role in the global transition toward sustainable and renewable energy sources. Accurately assessing its full potential requires a robust mathematical framework that adequately accounts for the Earth's curvature as well as large-scale atmospheric dynamics. Many traditional studies rely on Cartesian coordinate systems, which are well suited for local or regional analyses but may fail to capture the complex spatial variability of wind behavior on a planetary scale [1]. To overcome these limitations, this study adopts a spherical coordinate system (r,θ,ϕ), which provides a more physically consistent representation of wind energy distribution across different regions of the Earth. The theoretical investigation focuses on the derivation of fundamental equations governing wind power potential in spherical geometry, incorporating probabilistic models of wind speed and methods for estimating wind energy density over diverse geographical locations.

Analyzing wind energy potential using spherical coordinates improves the accuracy of global-scale theoretical models and enhances the understanding of atmospheric wind patterns. Moreover, this approach has important practical implications, including the optimization of wind farm placement, large-scale resource assessment, and the development of more effective global energy planning strategies [2].

This research seeks to bridge the gap between theoretical modeling and real-world applications by providing a solid scientific foundation for more efficient and sustainable utilization of wind energy on a global scale.

At present, the depletion of conventional energy resources such as oil, natural gas, and coal has become a critical global concern. Consequently, modern scientific and engineering research is increasingly focused on the development and implementation of alternative and renewable energy sources [4]. Among these alternatives, wind energy occupies a prominent position due to its wide availability and environmentally friendly nature.

A wide range of wind energy conversion systems has been designed and implemented to harness this resource, with modern wind turbines achieving efficiency levels of up to approximately 40% of the available wind energy. However, the successful design, placement, and operation of wind power plants require a thorough assessment of the atmospheric energy potential and regional wind characteristics [2; 3–5]. Accurate evaluation of these factors is essential for maximizing energy output and ensuring the long-term viability of wind energy projects.

International Journal of Advanced Research in Science, Engineering and Technology
Vol. 12, Issue 12, December 2025
ISSN: 2350-0328
IJARSET IMPACT FACTOR 7.150

II. RELATED WORK

Wind energy assessment is primarily conducted using meteorological measurement equipment, and the collected data serve as the basis for determining the optimal placement of wind generators and wind power plants [6; 9–11]. Despite significant progress in experimental and numerical studies, there is currently no comprehensive theoretical model that directly determines wind speed and wind power distribution within a global Earth-based coordinate system.

The development of a theoretical model for wind speed expressed in Earth's coordinates would make it possible to predict the locations and characteristics of experimental measurement points in advance, thereby improving the efficiency of wind resource assessment. Furthermore, meteorological observations frequently reveal pronounced peak-like variations in wind speed, the physical origins of which are not yet fully explained within existing theoretical frameworks.

Consequently, the statistical analysis and theoretical formulation of a wind flow formation model that accounts for these observed phenomena are of high scientific relevance. Such a model would contribute to a deeper understanding of atmospheric dynamics and support more accurate prediction and optimization of wind energy resources.

III. SIGNIFICANCE OF THE SYSTEM

In this article, a theoretical model is developed to determine wind energy potential at various locations on the Earth by analytically defining wind energy and its potential using coordinate-based theoretical calculations and mathematical formulations. The study focuses on investigating wind potential and improving the efficiency of its utilization through a comprehensive theoretical analysis.

Related works by other researchers are reviewed in Section II, the methodology is presented in Section IV, the experimental results and discussion are analyzed in Section V, and future research directions and conclusions are discussed in Section VI.

IV. METHODOLOGY

To design the generated capacities from the wind, it is necessary to consider that the system will use wind vane-type generators, which allow adjusting their position in the direction of the wind, aligning with the maximum wind speed [7–8; 12]. Therefore, a relationship is established between wind speed and generated power, where the total power received is equal to the product of the kinetic energy of the entire wind flow and the wind speed (1), with transformations.

$$P = \frac{mv^2}{2} * v = \frac{1}{2}\rho S h v^3 \tag{1}$$

The resulting expression includes the atmospheric air density, the height of the energy reception point, and the wind speed. In the present analysis, the height of the atmospheric layer under consideration and the air density may be assumed constant, while the effective area can be determined from the given geometric parameters of the system. Under these assumptions, the primary variable influencing the generated power is the wind speed.

Wind speed, in turn, is influenced by atmospheric temperature variations. To account for this dependence, the atmospheric system of the Earth can be approximated as isochoric, assuming a constant volume of air on a planetary scale. Under isochoric conditions, the ratios between the relevant thermodynamic quantities remain constant, leading to the following proportional relationship:

$$\frac{p_1}{T_1} = \frac{p_2}{T_2} => p_2 = \frac{p_1 T_2}{T_1} = \frac{F}{S} = \frac{mv}{St} => v = \frac{p_1 T_2 S t}{m T_1} = \frac{p_1 T_2 t}{\rho h T_1} \tag{2}$$

In this case, the initial pressure value is equal to atmospheric pressure, and temperature values can be determined based on the temperature difference between two specified points. Additionally, temperature variation depends on time. To calculate temperature formation, a model of uneven energy transfer from the Sun to the planet is used [13] (3).

$$E(\varphi_1, \varphi_2, t) = -1.41 * 10^{85} \left(9.872255241 * 10^{11}\varphi_1^2 + 7{,}431625476 * 10^{19}\varphi_1 + e\right)$$
$$* \left(e - \left(\begin{matrix}3.984197446 * 10^{51}\varphi_2^2 + 3.113172041 * 10^{60}\varphi_2 \\ -1.082173143 * 10^{55}\end{matrix}\right)\sin^2\varphi_2\right) *$$
$$1\,296.242207 e^{3.424889612 * 10^{-19} t_1} \tag{3}$$

When using the specified function that depends on coordinates in a spherical coordinate system, as well as on additional time starting from the Sun's origin, the temperature value (4) can be obtained.

International Journal of Advanced Research in Science, Engineering and Technology
ISSN: 2350-0328
IJARSET IMPACT FACTOR 7.150
Vol. 12, Issue 12, December 2025

$$Q = cm\Delta t => \Delta t = \frac{Q}{cm} => T_{(4)} = \frac{\frac{1}{4}\sum_{i=1}^{4} E_i(\varphi_{1i}, \varphi_{2i}, t)}{c_{atm}\rho_{atm} h S_{(4)}} \quad (4)$$

The formula incorporates the area of a curved quadrilateral on the surface of a sphere, which is also considered in the original equations. Based on all the transformations, a unified expression for wind speed (5) can be derived.

$$v = \frac{p_1(\frac{1}{4}\sum_{i=1}^{4} E_i(\varphi_{1i}, \varphi_{2i}, t)\, t}{\rho h \frac{\frac{1}{4}\sum_{j=1}^{4} E_j(\varphi_{1j}, \varphi_{2j}, t)}{c_{atm}\rho_{atm} h S_{(4)}}}$$
$$= \frac{t S_{(4)2} p_1(\frac{1}{4}\sum_{i=1}^{4} E_i(\varphi_{1i}, \varphi_{2i}, t))}{\rho_{atm} S_{(4)1} h(\frac{1}{4}\sum_{j=1}^{4} E_j(\varphi_{1j}, \varphi_{2j}, t))} \quad (5)$$

To determine the area on the surface of a sphere (O, R), the following geometric modeling is necessary. In the problem being formed, the ABCD quadrilateral has 4 points on the surface of the sphere with known coordinates of latitude, longitude and radius, forming a spherical coordinate system $(r, \varphi_1, \varphi_2)$. When projected from the surface of the sphere onto a plane, the curved quadrilateral transforms into a rectangle. The quadrilateral ABCD consists of four arcs — $\overset{\frown}{AB}$, $\overset{\frown}{BC}$, $\overset{\frown}{CD}$ and $\overset{\frown}{AD}$ on each of its sides.

The area of the formed rectangle ABCD is calculated based on the difference in angular coordinates. Thus, when analyzed in terms of the section and the given coordinates of all four points - $(r_1, \varphi_{11}, \varphi_{12}), (r_2, \varphi_{21}, \varphi_{22}), (r_3, \varphi_{31}, \varphi_{32}), (r_4, \varphi_{41}, \varphi_{42})$, the difference in radii allows them to be transformed as $(\varphi_{11}, \varphi_{12}), (\varphi_{21}, \varphi_{22}), (\varphi_{31}, \varphi_{32}), (\varphi_{41}, \varphi_{42})$. Another aspect to consider from the section's perspective is the possibility of determining the length of the segment between two coordinates, given the angle between two radii connected by an arc. This can be derived using the cosine rule in triangle AOB, between points A and B (6).

$$\begin{cases} \alpha_1 = \varphi_{21} - \varphi_{11} \\ \alpha_2 = \varphi_{22} - \varphi_{12} \end{cases}, \quad a^2 = b^2 + c^2 - 2bc\cos\alpha =>$$
$$=> \begin{cases} AB = CD = R\sqrt{2(1-\cos\alpha_1)} \\ BC = AC = R\sqrt{2(1-\cos\alpha_2)} \end{cases} \quad (6)$$

Therefore, the internal area of S_{ABCD} is (7).

$$S_{ABCD} = 2R^2(1-\cos\alpha_1)(1-\cos\alpha_2) \quad (7)$$

To calculate the area of the arcs, it is important to note that the height of the arc in the rectangle's projection is equal to the height of the arc in the section.

Therefore, calculating the circular segment in the projection can be reduced to determining the area of the corresponding projected segment of a rectangle on the plane. Since the length of the segment defined by the radius lines forming the arc is known and corresponds to one side of the rectangle, the problem is simplified. Under these conditions, the area of the projected segment can be directly evaluated using the circular segment area formula (8), which provides an efficient and sufficiently accurate means of calculating the required segment area.

$$\begin{cases} S_1 = \frac{1}{2}R^2\left(\frac{\pi\alpha_1}{180} - \sin\alpha_1\right) \\ S_2 = \frac{1}{2}R^2\left(\frac{\pi\alpha_2}{180} - \sin\alpha_2\right) \end{cases} \quad (8)$$

Based on this, the general area formula is (9).

$$S = R^2\left(2(1-\cos(\alpha_1))(1-\cos(\alpha_2)) + \left(\frac{\pi\alpha_1}{180} - \sin\alpha_1\right) + \left(\frac{\pi\alpha_2}{180} - \sin\alpha_2\right)\right) =$$
$$= R^2\begin{pmatrix} 2(1-\cos(\varphi_{21}-\varphi_{11}))(1-\cos(\varphi_{22}-\varphi_{12})) + \\ + \left(\frac{\pi(\varphi_{21}-\varphi_{11})}{180} - \sin(\varphi_{21}-\varphi_{11})\right) + \\ + \left(\frac{\pi(\varphi_{22}-\varphi_{12})}{180} - \sin(\varphi_{22}-\varphi_{12})\right) \end{pmatrix} \quad (9)$$

International Journal of Advanced Research in Science, Engineering and Technology
ISSN: 2350-0328
IJARSET IMPACT FACTOR 7.150
Vol. 12, Issue 12, December 2025

As a result of substituting the obtained area expressions into the velocity expression in (5), the complete velocity formula (10) is derived.

$$v = \frac{tp_1R^2}{\rho_{atm}h} * \sum_{i=1}^{4} \frac{E_{1i}(\varphi_{1i}, \varphi_{1i}, t)}{E_{2i}(\varphi_{2i}, \varphi_{2i}, t_1)} * \\ * \begin{pmatrix} 2(1-\cos(\varphi_{21}-\varphi_{11}))(1-\cos(\varphi_{22}-\varphi_{12})) + \\ + \left(\frac{\pi(\varphi_{21}-\varphi_{11})}{180} - \sin(\varphi_{21}-\varphi_{11})\right) + \\ + \left(\frac{\pi(\varphi_{22}-\varphi_{12})}{180} - \sin(\varphi_{22}-\varphi_{12})\right) \end{pmatrix} * \\ * \begin{pmatrix} 2\left(1-\cos\left((\varphi_{21}+\Delta_1)-(\varphi_{11}+\Delta_2)\right)\right) * \\ * \left(1-\cos\left((\varphi_{22}+\Delta_1)-(\varphi_{12}+\Delta_2)\right)\right) + \\ + \left(\frac{\pi\left((\varphi_{21}+\Delta_1)-(\varphi_{11}+\Delta_2)\right)}{180} - \sin\left((\varphi_{21}+\Delta_1)-(\varphi_{11}+\Delta_2)\right)\right) + \\ + \left(\frac{\pi\left((\varphi_{22}+\Delta_1)-(\varphi_{12}+\Delta_2)\right)}{180} - \sin\left((\varphi_{22}+\Delta_1)-(\varphi_{12}+\Delta_2)\right)\right) \end{pmatrix}^{-1} \quad (10)$$

The final stage of substitution is the derivation of the expression for the kinetic energy generated by wind generators (11).

$$P = \frac{1}{2}\rho h R^2 \begin{pmatrix} 2(1-\cos(\varphi_{21}-\varphi_{11}))(1-\cos(\varphi_{22}-\varphi_{12})) + \\ + \left(\frac{\pi(\varphi_{21}-\varphi_{11})}{180} - \sin(\varphi_{21}-\varphi_{11})\right) + \\ + \left(\frac{\pi(\varphi_{22}-\varphi_{12})}{180} - \sin(\varphi_{22}-\varphi_{12})\right) \end{pmatrix}^{3} * \\ * \begin{pmatrix} 2\left(1-\cos\left((\varphi_{21}+\Delta_1)-(\varphi_{11}+\Delta_2)\right)\right) * \\ * \left(1-\cos\left((\varphi_{22}+\Delta_1)-(\varphi_{12}+\Delta_2)\right)\right) + \\ + \left(\frac{\pi\left((\varphi_{21}+\Delta_1)-(\varphi_{11}+\Delta_2)\right)}{180} - \sin\left((\varphi_{21}+\Delta_1)-(\varphi_{11}+\Delta_2)\right)\right) + \\ + \left(\frac{\pi\left((\varphi_{22}+\Delta_1)-(\varphi_{12}+\Delta_2)\right)}{180} - \sin\left((\varphi_{22}+\Delta_1)-(\varphi_{12}+\Delta_2)\right)\right) \end{pmatrix}^{-3} * \\ * \left(\frac{tp_1R^2}{\rho_{atm}h} * \sum_{i=1}^{4} \frac{E_i(\varphi_{1i}, \varphi_{1i}, t)}{E_i(\varphi_{1i}+\Delta_1, \varphi_{1i}+\Delta_2, t_1)}\right)^{3} * \\ * \begin{pmatrix} 2(1-\cos(\varphi_{21}-\varphi_{11}))(1-\cos(\varphi_{22}-\varphi_{12})) + \\ + \left(\frac{\pi(\varphi_{21}-\varphi_{11})}{180} - \sin(\varphi_{21}-\varphi_{11})\right) + \\ + \left(\frac{\pi(\varphi_{22}-\varphi_{12})}{180} - \sin(\varphi_{22}-\varphi_{12})\right) \end{pmatrix}^{3} * \\ * \begin{pmatrix} 2\left(1-\cos\left((\varphi_{21}+\Delta_1)-(\varphi_{11}+\Delta_2)\right)\right) * \\ * \left(1-\cos\left((\varphi_{22}+\Delta_1)-(\varphi_{12}+\Delta_2)\right)\right) + \\ + \left(\frac{\pi\left((\varphi_{21}+\Delta_1)-(\varphi_{11}+\Delta_2)\right)}{180} - \sin\left((\varphi_{21}+\Delta_1)-(\varphi_{11}+\Delta_2)\right)\right) + \\ + \left(\frac{\pi\left((\varphi_{22}+\Delta_1)-(\varphi_{12}+\Delta_2)\right)}{180} - \sin\left((\varphi_{22}+\Delta_1)-(\varphi_{12}+\Delta_2)\right)\right) \end{pmatrix}^{-3} \quad (11)$$

International Journal of Advanced Research in Science, Engineering and Technology
ISSN: 2350-0328
Vol. 12, Issue 12, December 2025

As a result, a single function was obtained that depends on multiple variables, allowing for the modeling of generated wind power values.

V. EXPERIMENTAL RESULTS AND DISCUSSION

To create a graph of such a function, several stages of computation are required. The value of the detected areas per unit of the longitudinal section remains constant, based on which the detected area is determined. When calculated for the entire Earth, this value is 4,179.005 km², forming an imaginary rectangle with a side length of 64.64522 km (these data are determined based on the minimum calculation possibilities). The next value is the energy function values for the first and second stages, which differ due to variations in the input angle values at the selected time (Figure. 1-2).

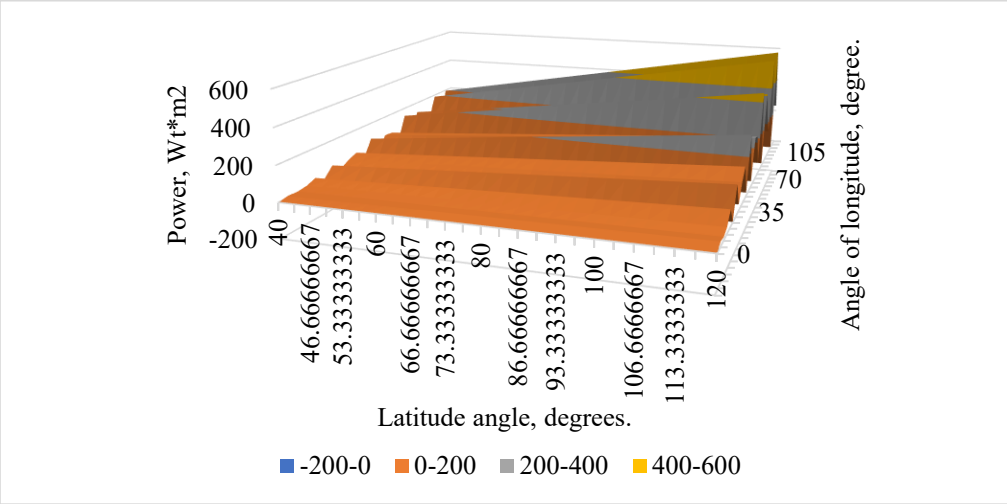

Figure. 1. ***Power graph in three-dimensional coordinates at the first calculation point.***

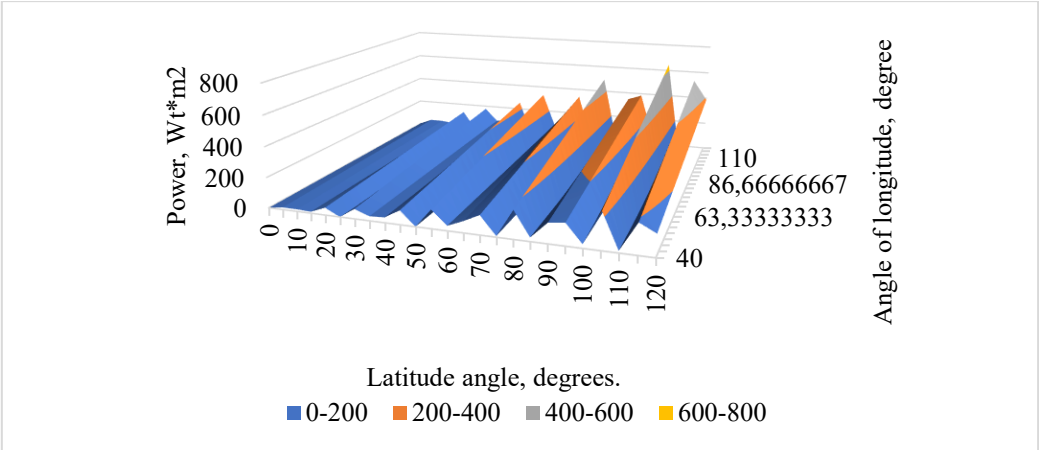

Figure. 2. ***Power graph in three-dimensional coordinates at the second calculation point.***

The resulting graphs indicate periodic bands of power variation along Earth's coordinates. It is assumed that the frequency of power fluctuations is related to changes between day and night at the selected calculation points. Based on the obtained power data, it is possible to generate a graph of wind speed variations according to Earth's coordinates for the specified calculation points (Figure. 3).

International Journal of Advanced Research in Science, Engineering and Technology
Vol. 12, Issue 12, December 2025
ISSN: 2350-0328
IJARSET IMPACT FACTOR 7.150

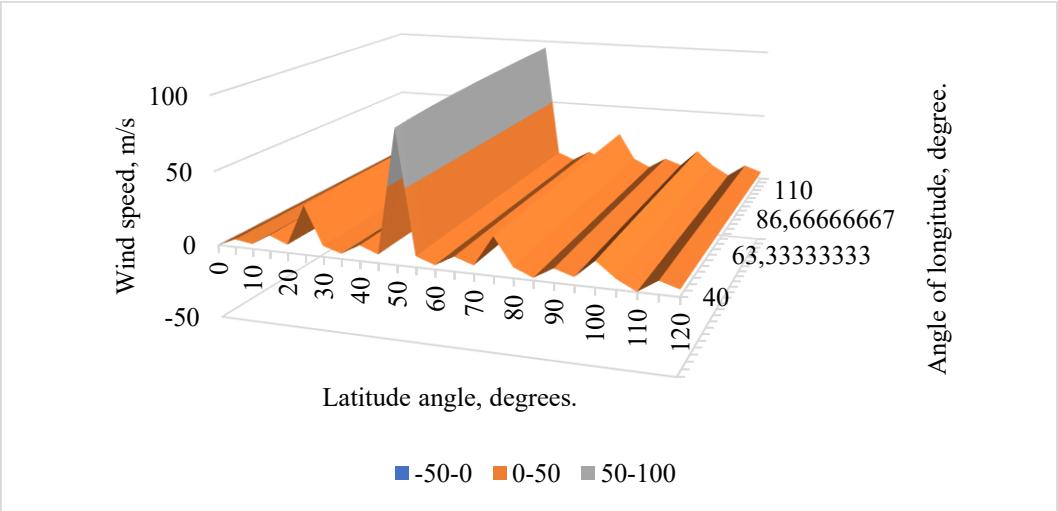

Figure. 3. ***Graph of wind speed in three-dimensional space.***

The obtained theoretical calculation results correlate with the actual wind speed graph (Figure. 4-5).

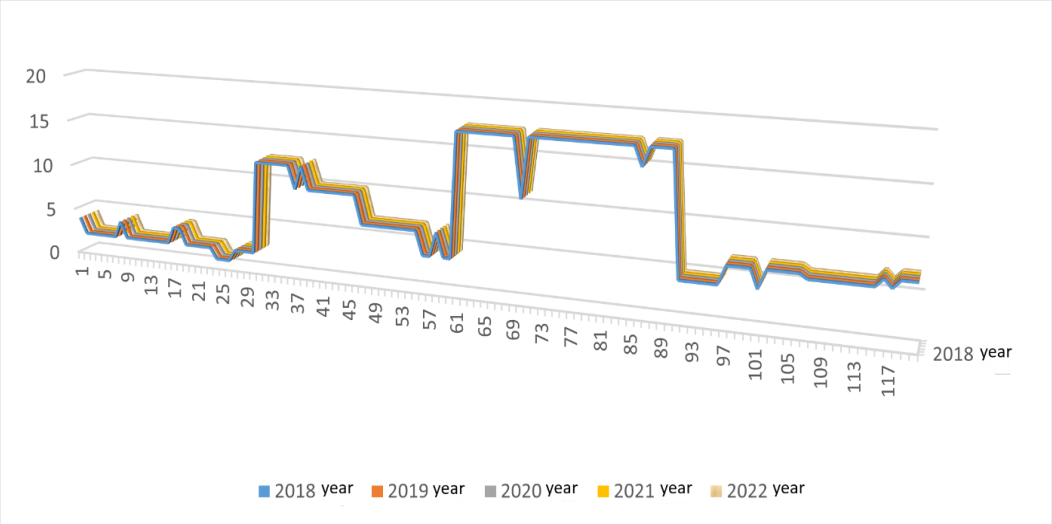

Figure. 4. ***Metrological data of wind speed for 5 years (2018-2022) [14-15]***

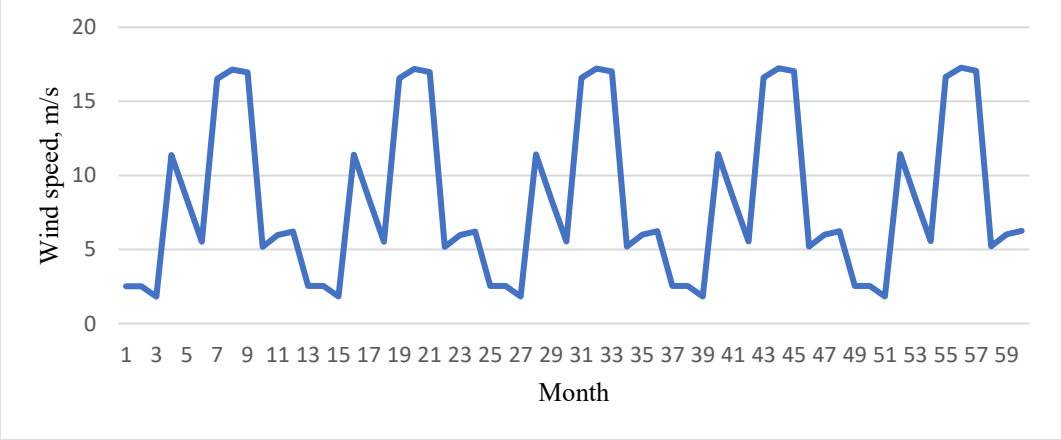

Figure. 5. ***Average monthly graph of values over a five-year period [14-15].***

International Journal of Advanced Research in Science, Engineering and Technology
ISSN: 2350-0328
Vol. 12, Issue 12, December 2025

The presented graphs are based on observations conducted by the meteorology center in the Fergana Valley over a period of five years, during which daily wind speed measurements were recorded. The final stage of modeling, based on the obtained results, includes plotting the wind power function. The values in the meteorological data may vary due to the influence of external factors. (Figure. 6).

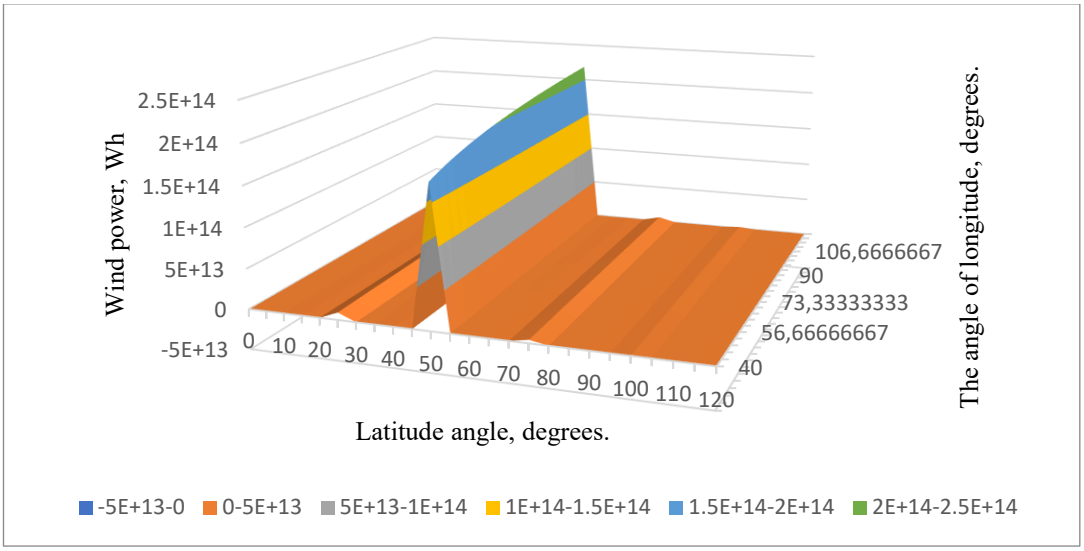

Figure. 6. ***Estimated wind power in three-dimensional space.***

V. CONCLUSION AND FUTURE WORK

Research confirms that the wind energy potential varies periodically depending on the Earth's coordinates. These fluctuations are associated with changes in atmospheric dynamics, wind directions, and temperature differences between day and night. In Uzbekistan, particularly in the Fergana region, the average wind speed ranges from 13 to 18 m/s, with a maximum speed reaching up to 25 m/s, indicating a high potential for wind energy utilization.
The research conclusions are as follows:

1. There is great potential for utilizing wind energy in Uzbekistan.
2. The most suitable areas for constructing wind power plants have been identified.
3. A specific theoretical model has been developed to analyze the wind energy potential in the Fergana region.
4. This model enables the prediction of the geographic distribution of wind energy.
5. It supports strategic decision-making for the optimal placement of wind power plants.

This study, based on future theoretical and practical work, establishes a scientific foundation for understanding wind energy potential through a spherical coordinate-based model and offers a more precise tool for optimizing wind energy utilization.
According to the model's predictions, global wind energy resources could provide up to 18 MW annually, which would be sufficient to partially meet Uzbekistan's primary energy demand.
The practical implementation of these research findings could increase wind energy efficiency by 15–30%, reduce infrastructure costs by 10–20%, and minimize environmental impacts by 30–40%.

REFERENCES

1. Weather-sensitive renewable energy sources do not subject power systems to blackouts. Nat Energy 9, 1331–1332 (2024). https://doi.org/10.1038/s41560-024-01657-w
2. Parker, D.P., Johnston, S., Leonard, B. et al. Economic potential of wind and solar in American Indian communities. Nat Energy 9, 1360–1368 (2024). https://doi.org/10.1038/s41560-024-01617-4
3. Zhao, J., Li, F. & Zhang, Q. Impacts of renewable energy resources on the weather vulnerability of power systems. Nat Energy 9, 1407–1414 (2024). https://doi.org/10.1038/s41560-024-01652-1
4. de Kleijne, K., Huijbregts, M.A.J., Knobloch, F. et al. Author Correction: Worldwide greenhouse gas emissions of green hydrogen production and transport. Nat Energy 9, 1449 (2024). https://doi.org/10.1038/s41560-024-01644-1
5. Thurstan, R.H., McCormick, H., Preston, J. et al. Records reveal the vast historical extent of European oyster reef ecosystems. Nat Sustain (2024). https://doi.org/10.1038/s41893-024-01441-4
6. Shankar, M., Ng, M., Rogers, M. et al. Unearthing the role of soils in urban climate resilience planning. Nat Sustain 7, 1374–1376 (2024). https://doi.org/10.1038/s41893-024-01436-1

7. Burger, M.N., Mahabadi, D. & Vollan, B. Technology-minded climate delegates support less stringent climate policies. Nat Sustain 7, 1405–1408 (2024). https://doi.org/10.1038/s41893-024-01434-3
8. Zhong, H., Li, Y., Ding, J. et al. Global spillover effects of the European Green Deal and plausible mitigation options. Nat Sustain 7, 1501–1511 (2024). https://doi.org/10.1038/s41893-024-01428-1
9. Wollburg, P., Markhof, Y., Bentze, T. et al. Substantial impacts of climate shocks in African smallholder agriculture. Nat Sustain 7, 1525–1534 (2024). https://doi.org/10.1038/s41893-024-01411-w
10. Shuni Wei, Peng Yuan, Renjie Yu. Can renewable portfolio standard promote renewable energy capacity utilization? Empirical evidence from China. Renewable and Sustainable Energy Reviews. Volume 210, March 2025, 115159. https://doi.org/10.1016/j.rser.2024.115159
11. Yanlai Zhou, Zhihao Ning, Kangkang Huang, Shenglian Guo, Chong-Yu Xu, Fi-John Chang. Sustainable energy integration: Enhancing the complementary operation of pumped-storage power and hydropower systems. Renewable and Sustainable Energy Reviews. Volume 210, March 2025, 115175. https://doi.org/10.1016/j.rser.2024.115175
12. Faraedoon Ahmed, Aoife Foley, Sean McLoone, Robert Best, Henrik Lund, Dlzar Al Kez. Sectoral coupling pathway towards a 100 % renewable energy system for Northern Ireland. Renewable and Sustainable Energy Reviews. Volume 210, March 2025, 114939. https://doi.org/10.1016/j.rser.2024.114939
13. N. R. Avezova, Ergashali Yuldashevich Rakhimov, Nargiza Dalmuradova, Semen Frid, Shermuhammad Muminov. “Assessment of the Technical Potential of Photovoltaic Convertors: The Case of the Fergana Valley Part I: Dynamics of Climate Data Changes in the Region” December 2022Applied Solar Energy 58(5):896-910.

AUTHOR’S BIOGRAPHY

Full name	**Ergashev Sirojiddin Fayazovich**
Science degree	DSc
Academic rank	Senior Researcher
Institution	Fergana state technical university Fergana, Uzbekistan

Full name	**Rakhimov Abdurakhmon Abduraufjon ugli**
Science degree	-
Academic rank	PhD student
Institution	Fergana state technical university Fergana, Uzbekistan